1   **Aerosol pH and its influencing factors in Beijing**

2   **Jing Ding[2, 1], Pusheng Zhao[1, 3*], Jie Su[1], Qun Dong[1], and Xiang Du[1]**

3   [1] Institute of Urban Meteorology, China Meteorological Administration, Beijing 100089, China

4   [2] State Environmental Protection Key Laboratory of Urban Ambient Air Particulate Matter Pollution

5   Prevention and Control, College of Environmental Science and Engineering, Nankai University,

6   Tianjin 300071, China

7   [3] Max Planck Institute for Chemistry, Mainz 55128, Germany

8   *** *Correspondence to:* P. S. Zhao (pszhao@ium.cn)

9   **Abstract**

10   Acidity (pH) plays a key role in the physical and chemical behavior of aerosol and cannot be

11   measured directly. In this work, aerosol liquid water content (ALWC) and size-resolved pH are

12   predicted by thermodynamic model (ISORROPIA-II) in 2017 of Beijing. The mean aerosol pH over

13   four seasons is 4.3±1.6 (spring), 4.5±1.1 (winter), 3.9±1.3 (summer), 4.1±1.0 (autumn), respectively,

14   showing the moderate aerosol acidity. The aerosol pH in fine mode is in the range of 1.8 ~ 3.9, 2.4

15   ~ 6.3 and 3.5 ~ 6.5 for summer, autumn and winter, respectively. And coarse particles are generally

16   neutral or alkaline. Diurnal variation of aerosol pH follows both aerosol components (especially the

17   sulfate) and ALWC. For spring, summer and autumn, the averaged nighttime pH is 0.3~0.4 unit

18   higher than that on daytime. Whereas in winter, the aerosol pH is relatively low at night and higher

19   at sunset. SO_4^{2-} and RH are two crucial factors affecting aerosol pH. For spring, winter and autumn,

20   the effect of SO_4^{2-} on aerosol pH is greater than RH, and it is comparable with RH in summer. The

21   aerosol pH decreases with elevated SO_4^{2-} concentration. As the NO_3^- concentration increases, the

22   aerosol pH firstly increases and then decreases. Sulfate-dominant aerosols are more acidic with pH

23   lower than 4, whereas nitrate-dominated aerosols are weak in acidity with pH ranges 3~5. In recent

24   years, the dominance of NO_3^- in inorganic ions may be another reason responsible for the

25   moderately acidic aerosol. ALWC has a different effect on aerosol pH in different seasons. In winter,

26   the increasing RH could reduce the aerosol pH whereas it shows a totally reverse tendency in

27   summer, and the elevated RH has little effect on aerosol pH in spring and autumn when the RH is

28   between 30% and 80%. The dilution effect of ALWC on H_{air}^+ is only obvious in summer. The

29   elevated NH_3 and NH_4^+ could reduce aerosol acidity by decreasing H_{air}^+ concentration exponentially.

30   ***Key words:*** Aerosol pH, Size distribution, Influening factors, Beijing

1. Introduction

Acidity or pH, which drives many processes related to particle composition, gas-aerosol partitioning and aerosol secondary formation, is an important aerosol property (Jang et al., 2002; Eddingsaas et al., 2010; Surratt et al., 2010). The aerosol acidity has a significant effect on the aerosol secondary formation through the gas-aerosol partitioning of semi-volatile and volatile specials (Pathak et al., 2011a; Guo et al., 2016). Recent studies have shown that aerosol acidity could promote the generation of secondary organic aerosol by affecting the aerosol acid-catalyzed reactions (Rengarajan et al., 2011;). Moreover, metals can become soluble by acid dissociation under lower pH conditions (Shi et al., 2011; Meskhidze et al., 2003) or by forming a ligand with organic species, such as oxalate at higher pH (Schwertmann et al., 1991). In addition, higher aerosol acidity could lower the acidification buffer capacity and affect the formation of acid rain. The investigation in aerosol acidity is conducive to better understand the important role of aerosols in acid deposition and atmospheric chemical reactions.

The hygroscopic components in the aerosols include water-soluble inorganic ions and part of organic acid (Peng, 2001; Wang et al., 2017). The deliquescence relative humidity for the mixed-salt is lower than that of any one component (Seinfeld and Pandis, 2016), hence the ambient aerosols are generally droplets containing liquid water. The aerosol pH actually is the pH of the aerosol liquid water. The aerosol acidity is usually estimated by the charge balance of measurable cations and anions. A net negative balance correlated with an acidic aerosol and vice versa (Zhang et al., 2007; Pathak et al., 2011b; Zhao et al., 2017). Generally, a larger value of the ion balance implies a stronger acidity or stronger alkaline. Nevertheless, an ion balance or other similar proxies fail to represent the true aerosol pH because the aerosol acidity estimated by this way is measured through the aerosol water extract, which poorly predicts the concentration of hydronium ion in the aerosol liquid water (Guo et al., 2015; Hennigan et al., 2015). Moreover, due to the large amounts of water is used for extraction, the results cannot reflect the characteristics of the in-situ aerosol acidity, and it cannot be applied to study the influence of aerosol acidity on gas-particle conversion. In-situ aerosol acidity, defined as the free H^+ concentration in the liquid phase of a particle, is an important parameter that actually affects the chemical behavior of the particle, which could be calculated by hydrogen ion concentration and the aerosol liquid water content (ALWC).

61   It is critical to obtain the ALWC in calculating aerosol acidity. One way to calculate the ALWC

62   is based upon the assumption that the volume of ALWC is equal to subtracting the volume of dry

63   aerosol particles from that of wet particles (Guo et al., 2015; Bian et al. 2014; Engelhart et al. 2011).

64   Under this assumption, ALWC could be calculated by the size-resolved hygroscopic growth factors

65   (g(D, RH)) combining particle size distribution (PNSDs) or by the hygroscopic growth factor of

66   aerosol scattering coefficient (f(RH)) (Bian et al. 2014; Guo et al., 2015; Kuang et al., 2017a). The

67   g(D, RH), defined as the ratio of the diameter of the wet particle at a certain relative humidity to the

68   corresponding diameter at dry conditions, could be measured by H-TDMA (Hygroscopic Tandem

69   Differential Mobility Analyzer) (Liu et al., 1978; Swietlicki et al., 2008; Liu et al., 2011). And the

70   f(RH) could be observed by the wet & dry nephelometer system (Covert et al., 1972; Rood et al.

71   1985; Yan et al., 2009; Kuang et al., 2016, 2017b).

72   Another way to calculate the ALWC is based on the aerosol chemical components with

73   thermodynamic models, such as ISORROPIA-II, AIM, ADDEM etc. (Nenes et al., 1998;

74   Fountoukis and Nenes, 2007, Clegg et al., 1998, Topping et al., 2005a, b). Based on the aerosol

75   chemical components as well as temperature and relative humidity, the aerosol thermodynamic

76   models could output both ALWC and concentration of the hydronium ion in air (moles H^+ per

77   volume of air, denoted hereafter as H_{air}^+), which offers a more precise approach to acquire aerosol

78   pH (Pye et al., 2013). Among these thermodynamic models, ISORROPIA and ISORROPIA-II are

79   most widely used owing to its rigorous calculation and performance on computational speed.

80   ISORROPIA simulates the gas-particle partitioning in the H_2SO_4, NH_3, HNO_3, HCl, Na^+, H_2O

81   system, while its second version, ISORROPIA-II, adds Ca^{2+}, K^+, Mg^{2+} and the corresponding salts

82   to the simulated particle components in thermodynamic equilibrium with water vapor and gas-phase

83   precursors.

84   Comparisons were made in some studies to investigate the consistency of calculated ALWC

85   derived from the above methods. In the North China Plain, Bian et al. (2014) found that the ALWC

86   calculated using size-resolved hygroscopic growth factors and the PNSD agreed well with that

87   calculated using ISORROPIA II at higher relative humidity (>60%). Relatively good consistency

88   was also found in the study of Engelhart et al. (2011) in USA based on the similar method. Guo et

89   al. (2015) compared the ALWC calculated by f (RH) with the total predicted water by organics and

90   inorganics. The total predicted water was highly correlated and on average within 10 % of the f(RH)

91   measured water. Though good consistencies in ALWC were found among these methods, the H_{air}^+

92   could only be obtained by thermodynamic models, which have been applied to predict aerosol

93   acidity in many studies (Nowak et al., 2006; Fountoukis et al., 2009; Weber et al., 2016; Fang et al.,

94   2017).

95   When calculating aerosol acidity with thermodynamic models, the aerosol is assumed internally

96   mixed and the bulk properties of aerosol are used, without considering variability of chemical

97   compositions with particle size. However, the size-resolved characteristics of aerosol chemical

98   components are obviously different. Among inorganic ions, SO_4^{2-}, NO_3^-, Cl^-, K^+, NH_4^+ are mainly

99   concentrated in fine mode, whereas Mg^{2+}, Ca^{2+} are abundant in coarse mode (Zhao et al., 2017). The

100   aerosol acidity is the result of the balance between the soluble acidic (SO_4^{2-}, NO_3^-, Cl^- and some

101   soluble organic acids) and alkaline (NH_4^+, Na^+, K^+, Mg^{2+}, Ca^{2+}) component in the aerosol. The gas

102   precursor NH_3, HNO_3, and HCl for main water-soluble ions as well as ambient temperature and

103   relative humidity are also important factors affecting the aerosol acidity. In some countries where

104   PM concentration is very low, the pH diurnal variation was mainly driven by meteorological

105   conditions (Guo et al., 2015, 2016; Bougiatioti et al., 2016). In China, however, the annual average

106   $PM_{2.5}$ concentration in some mega cities was ~2 times higher than the national standard value (35

107   $\mu g\ m^{-3}$) and the inorganic ions account for 40%~50% to $PM_{2.5}$, especially in the North China Plain

108   (Zou et al., 2018; Huang et al., 2017; Gao et al., 2018). Hence it can be expected that the aerosol

109   composition is also a crucial factor on pH, which cannot be ignored.

110   The North China Plain is the region with the most severe aerosol pollution in China. Nevertheless,

111   few studies have focused on aerosol pH at this region. Cheng et al. (2016) estimated the averaged

112   pH by ISORROPIA-II, and Wang et al. (2016) derived the particle pH by using a molar ratio

113   approach in Beijing, their results show that the aerosol acidity was close to neutral. However, Liu

114   et al. (2017) and Shi et al. (2017) found that fine particles in the North China Plain were moderately

115   acidic based on the hourly measured particulate water-soluble ions and precursor gases along with

116   ISORROPIA-II, with an average pH of 4.2 in winter of Beijing and 4.9 in Tianjin. These results are

117   all significantly higher than that in the United States or Europe, where aerosols are often highly

118   acidic with a pH lower than 3.0 (Guo et al., 2015, 2016; Bougiatioti et al., 2016; Weber et al., 2016;

119   Young et al., 2013). The differences in aerosol pH in the North China Plain mainly result from the

120   different calculated methods (ion balance & thermodynamic equilibrium models). Several studies

121   have shown that the ion balance and reverse-mode calculations of thermodynamic equilibrium

122   models are not applicable to interpret the aerosol acidity (Hennigan et al., 2015; Liu et al. 2017;

123   Song et al., 2018). Moreover, the change of the chemical composition of $PM_{2.5}$ in the North China

124   Plain in recent years also contributed to the differences in aerosol pH. The observations in previous

125   studies exploring aerosol acidity in the North China Plain were almost conducted before 2015. In

126   the recent three years, the chemical composition of $PM_{2.5}$ in Beijing has undergone tremendous

127   changes. Nitrate has replaced sulfate and is dominant in inorganic ions in most cases (Zhao et al.,

128   2017; Huang et al., 2017; Ma et al., 2017). Moreover, studies about seasonal variation of aerosol

129   pH and size-resolved aerosol pH are rare in the North China Plain, and the key factors affecting

130   aerosol acidity are still not well understood.

131   In this work, thermodynamic model ISORROPIA-II with forward mode is utilized to predict

132   ALWC and aerosol pH in Beijing. The hourly measured $PM_{2.5}$ inorganic ions and precursor gases

133   in four seasons during 2016 to 2017 are used to analyze the seasonal and diurnal variation of aerosol

134   acidity, and the sensitivity analysis is conducted to identify the key factors that affecting the aerosol

135   pH. In our previous studies, the multi-stage cascade impactors (MOUDI-122) were used for size-

136   resolved aerosol sampling during 2013 to 2015. The actual relative humidity inside the impactors

137   was calculated, and the size distribution of water-soluble ions, organic carbon, and elemental carbon

138   in three seasons were discussed (Zhao et al., 2017; Su et al., 2018). Based on these size-resolved

139   results, the pH for aerosol in different size ranges could also be modeled, which can help to evaluate

140   whether it is appropriate to calculate the overall pH of $PM_{2.5}$ ignoring the differences in particle size.

141   **2. Data Collection and Methods**

142   **2.1 Site**

143   The measurements were performed at the Institute of Urban Meteorology in Haidian district of

144   Beijing (39°56'N, 116°17'E). The sampling site was located next to a high-density residential area,

145   without significant air pollution emissions around the site. Therefore, the observation data could

146   represent the air quality levels of the urban area of Beijing.

147   **2.2 Online data collection**

148   Water-soluble ions (SO_4^{2-}, NO_3^-, Cl^-, NH_4^+, Na^+, K^+, Mg^{2+}, Ca^{2+}) of $PM_{2.5}$ and trace gases (HCl,

149   HNO_3, HNO_2, SO_2, NH_3) in the ambient air were measured by an online analyzer (MARGA) at

150   hourly temporal resolution during the spring (April and May in 2016), winter (February in 2017),

151   summer (July and August in 2017) and autumn (September and October in 2017). The more details

152   about MARGA can be found at ten Brink et al. (2007). The $PM_{2.5}$ and PM_{10} mass concentrations

153   (TEOM 1405DF), the hourly ambient temperature and relative humidity were also synchronously

154   attained.

155   Hourly concentrations of $PM_{2.5}$, PM_{10}, and water-soluble ions in $PM_{2.5}$, as well as meteorological

156   parameters during the observation, are shown in Figure 1. In spring, two dust events occurred (21-

157   22, April and 5-6, May). During the first dust event, the wind came predominantly from the north

158   with mean wind speed 3.5 m s^{-1}. And the PM_{10} concentration reached 425 µg m^{-3} while the $PM_{2.5}$

159   concentration was only 46 µg m^{-3} on the peak hour. Similarly, the second dust event was resulted

160   from the strong wind come from the northwest direction. In the following pH analysis based on

161   MARGA data, it is assumed that the particles were internally mixed, and the chemical compositions

162   were the same for particles of different sizes in $PM_{2.5}$. Hence, these two dust events were excluded

163   from this analysis.

164   **2.3 size-resolved chemical compositions**

165   A Micro-Orifice Uniform Deposit Impactor (MOUDI-120) was used to collect size-resolved

166   aerosol samples with the calibrated 50% cut sizes of 0.056, 0.10, 0.18, 0.32, 0.56, 1.0, 1.8, 3.1, 6.2,

167   9.9 and 18 µm. Size-resolved sampling was conducted during July 12-18, 2013; January 13-19,

168   2014; July 3-5, 2014; October 9-20, 2014; and January 26-28, 2015. Fifteen, fourteen, and eighteen

169   sets of samples were obtained for the summer, autumn and winter, respectively. Except for two sets

170   of samples, all the samples were collected in daytime (from 08:00 to 19:00) and nighttime (from

171   20:00 to 7:00 the next day), respectively. One hour of preparation time was set for filter changing

172   and nozzle plate washing with ethanol. The water-soluble ions were analyzed from the samples by

173   using an ion chromatography (DIONEX ICS-1000). The detailed information about the features of

174   MOUDI-120, the procedures of sampling, pre-treatment, and laboratory chemical analysis

175   (including the quality assurance & quality control) were described in our previous papers (Zhao et

176   al., 2017; Su et al., 2018).

2.4 Aerosol pH prediction

As mentioned in the Introduction, pH of ambient aerosols could be predicted by the thermodynamic model such as AIM and ISORROPIA, AIM is considered an accurate benchmark model while ISORROPIA has been optimized for use in chemical transport models. Currently, ISORROPIA-II, adds K^+, Mg^{2+}, Ca^{2+} (Fountoukis and Nenes, 2007), could calculate the equilibrium H_{air}^+ (particle hydronium ion concentration per volume air) and ALWC with reasonable accuracy by taking water-soluble ions mass concentration, temperature and relative humidity as input. The H_{air}^+ and ALWC were then used to predict aerosol pH by the Eq. (1).

$$\text{pH} = -\log_{10} H_{aq}^+ \cong -\log_{10} \frac{1000 H_{air}^+}{ALWC_i} \tag{1}$$

Where H_{aq}^+ (mole L^{-1}) is the hydronium ion concentration in the ambient particle liquid water. H_{aq}^+ can also be deemed to be the H_{air}^+ ($\mu g\ m^{-3}$) divided by the concentration of ALWC associated with inorganic species, $ALWC_i$ ($\mu g\ m^{-3}$). Both inorganic and part of organic species in particles are hygroscopic. However, the pH prediction is not highly sensitive to the water uptake by organic species ($ALWC_o$), unless the $ALWC_o$ mass fraction to the total particle water is close to 1 (Guo et al., 2015, 2016). And similar result was also found in Beijing in Liu et al. (2017). Hence the aerosol pH could be fairly predicted by ISORROPIA-II with just measurements of inorganic species in most cases.

In ISORROPIA-II, forward and reverse mode are provided to predict ALWC and H_{air}^+. In forward mode, known quantities are T, RH and the total (i.e. gas+aerosol) concentrations of NH_3, H_2SO_4, HCl and HNO_3. Reverse mode calculates the equilibrium partitioning given the concentration of only aerosol composition together with RH and T as input. In this work, the online ion chromatography MARGA was used to measure both inorganic ions of $PM_{2.5}$ and precursor gases, hence ISORROPIA-II was run in the "forward mode" for aerosols in metastable condition. Moreover, the forward mode was reported less sensitive to measurement error than the reverse mode (Hennigan et al., 2015; Song et al., 2018).

Running ISORROPIA-II in the forward mode with only aerosol concentrations as input may result in a bias in predicted pH due to repartitioning of ammonia in the model, leading to a lower predicted pH when gas-phase data are not available (Hennigan et al., 2015). In this work, no $NH_{3(g)}$

205 was available for the size-resolved pH prediction. We determined aerosol pH in the fine mode

206 through an iteration procedure that used the measured particulate species and ISORROPIA-II to

207 predict gas species, detailed information could be found in Fang et al. (2017) and Guo et al. (2017).

208 As for coarse mode particles, equilibrium is not considered between the gas and particles due to

209 kinetic limitations (Dassios et al., 1999; Cruz et al., 2000), the pH was determined by ignoring the

210 gas phase and ISORROPIA-II was run in forward mode with zero gas concentrations.

211 The accuracy of the aerosol pH prediction is primarily assessed by the reproduction of

212 semivolatile components partitioning between gas and particle phases. A comparison between

213 predicted NO_3^-, NH_4^+ and measured values colored by RH is shown in Figure 2. Overall, the model

214 captures the measured NO_3^-, NH_4^+, and the predicted NO_3^-, NH_4^+ are on average within ±20% of

215 the measurements, with R^2>0.9, and best agreement is observed at RH above 60%.

216

217 **Figure 1**

218

219 **3. Results and Discussion**

220 **3.1 Overall summary of aerosol pH over four seasons**

221 The averaged $PM_{2.5}$ concentration is 62±36, 60±69, 39±24, 59±48 μg m^{-3} in spring, winter,

222 summer and autumn observation, respectively. Among all ions measured, NO_3^-, SO_4^{2-}, NH_4^+ are

223 three dominant species, accounting for 83% ~ 87%. Compared with other seasons, the averaged

224 concentration of primary inorganic ions (Cl$^-$, Na$^+$, K$^+$, Mg^{2+}, Ca^{2+}) was higher in spring. The aerosol

225 in Beijing showed the moderate acidity with aerosol pH was 4.3±1.6, 4.5±1.1, 3.9±1.3 and 4.1±1.0

226 in spring, winter, summer and autumn observation, respectively. The overall winter aerosol pH is

227 comparable to the result found in Beijing (4.2, winter) from Liu et al. (2017) and lower than that

228 (4.9, winter and spring) in Tianjin (Shi et al., 2017), another mega city about 120 km away from

229 Beijing. The summer aerosol pH was lowest among all four seasons, implying the higher aerosol

230 acidity. The seasonal variation of aerosol pH in this work was similar to the result from Tan et al.

231 (2018) except for spring, which was winter (4.11 ± 1.37) > autumn (3.13 ± 1.20) > spring (2.12 ±

232 0.72) > summer (1.82 ± 0.53). Noted that the observation in Tan et al. (2018) was conducted in 2014

233 of Beijing, the distinction in aerosol composition may be responsible for the lower aerosol pH in

234   their work.

235   The acid liquid surface has a catalytic effect on the gas-liquid reaction process, and the presence

236   of the oxidant can significantly increase the reaction rate and promote the formation of secondary

237   aerosols (Liu et al., 2012). How the moderate acidity of aerosol in the North China Plain affect the

238   formation of secondary aerosols needs to be further investigated.

239   **Figure 2**

240   Wind dependence of $PM_{2.5}$, NO_3^-, SO_4^{2-}, NH_4^+, Ca^{2+} concentration and the averaged pH are shown

241   in Figure 3 and Fig. S1. In spring and summer, the high aerosol pH occurs with both NW and SW

242   strong winds (wind speed >3 m s^{-1}) while the low aerosol pH occurs with calm winds (wind speed

243   <2 m s^{-1}) and SW winds with wind speed lower than 3 m s^{-1}. For winter, we surprisingly found that

244   the high aerosol pH is mainly concentrated in the SSW direction, while the aerosol pH in northerly

245   winds is as low as 3~4. In autumn, the aerosol pH accompanied by NW winds is much higher than

246   that accompanied by souther winds. Generally, the northerly winds usually occur with cold front

247   systems and high wind speeds, which could sweep away air pollutants but raise dust in which the

248   crustal species (Ca^{2+}, Mg^{2+}) content are higher.

249   Haze episodes usually occur with SW and SE winds and calm winds in Beijing, the air pollutants

250   are transported to Beijing from other cities located in SW and SE directions, leading to the

251   accumulation of pollutants. Beijing is surrounded by mountains on three sides, and south Beijing is

252   plain. The industry is mainly concentrated in the south of Beijing, and there are plenty of emission

253   sources in these two major transport pathways from southwest and southeast directions, leading to

254   the higher $PM_{2.5}$ concentration. We find that the aerosol pH is negatively correlated with $PM_{2.5}$

255   concentration in spring, summer, and autumn whereas it shows the positive relationship in winter.

256   To further investigate the aerosol pH performance under different pollution level over four

257   seasons, the $PM_{2.5}$ concentration is classified into three groups with 0~75 μg m^{-3}, 75~150 μg m^{-3}

258   and >150 μg m^{-3}, representing clean, polluted and heavily polluted days, respectively. Overall, as

259   the air quality deteriorates, ALWC and H_{air}^+ all increased, but the aerosol acidity performs differently.

260   In spring, summer, and autumn, the pH on clean days is the highest (Table 1), then followed by

261   polluted days and heavily polluted days. In winter, however, the averaged pH on polluted days

262   (5.4±1.0) is the highest, then followed by heavily polluted days (4.4±0.9) and clean days (4.3±1.1).

263   **Figure 3**

264   **Table 1**

265

266   **3.2 Diurnal variation of aerosol pH, ALWC, and H_{air}^+**

267   The diurnal variation for ALWC is similar over four seasons, but distinctions are found in H_{air}^+

268   and pH diurnal variations (Figure 4). Generally, nighttime mean ALWC is higher than daytime and

269   reached a peak at near 04:00 ~ 06:00 (local time). After sunrise, the increasing temperatures resulted

270   in a rapid drop in RH, leading to the obvious loss of particle water, ALWC reached the lowest level

271   in the afternoon. For spring, summer, and autumn, the significant H_{air}^+ peak starting at roughly 12:00

272   and reaching a maximum between 16:00 and 18:00, the low ALWC and high H_{air}^+ resulted in the

273   minimum pH in the afternoon. The averaged nighttime pH is 0.3~0.4 unit higher than that on

274   daytime for spring, summer, and autumn, respectively. However, for winter, H_{air}^+ in the nighttime

275   is slightly higher than that in the daytime, and the aerosol pH is relatively low at night and higher at

276   sunset. Noted that the diurnal variation of aerosol pH is all consistent with the diurnal variation of

277   SO_4^{2-} over four seasons, it seems that the SO_4^{2-} is a key factor affecting aerosol pH.

278   **Figure 4**

279   The distinguishing diurnal patterns of aerosol pH over four seasons indicate that aerosol

280   composition is a key factor for the diurnal variation of aerosol pH, which is very different from what

281   Guo et al. (2015) found in the southeastern United States: the pH diurnal variation is largely driven

282   by meteorological conditions due to the dilution of ALWC to H_{air}^+, not aerosol composition. The

283   biggest reason for the discrepancy is that the hygroscopic components in particles such as

284     $(NH_4)_2SO_4$ and NH_4NO_3 in Beijing are much higher than that in the southeastern United States

285   (lower than 5 μg m^{-3}) while the mean RH is lower. Thus the influence of aerosol composition on pH

286   cannot be ignored in Beijing.

287   **3.3 Factors affecting ALWC, H_{air}^+ and aerosol pH**

288   As mentioned above, the aerosol chemical composition has a non-negligible effect on aerosol pH.

289   In this work, the effects of aerosol chemical components (NO_3^-, SO_4^{2-}, NH_4^+, Ca^{2+}) and precursor

290   gases (NH_3, HNO_3), as well as meteorological parameters (RH, T) on aerosol pH are performed

291 through a sensitivity analysis over four seasons. When assessing how a factor affects aerosol acidity,

292 ALWC, or H_{air}^+, the real-time measured values of an evaluated factor and the averaged values for

293 other factors in each season are input in ISORROPIA-II. For example, the magnitude of the

294 deviation for calculated aerosol pH can reflect the effect of an evaluated factor on the aerosol acidity.

295 The higher the deviation, the greater the effect, vice versa. Noted that the sensitivity analysis in this

296 work only reflects the characteristics during the observation period, further work is needed to

297 determine whether the sensitivity analysis is valid in other environments. And the sensitivity

298 analysis in this paper only focused on single factor variations, however, in reality, changes in one

299 factor could alter other factors and made it more complicated.

300  As show in Table 2, for ALWC, the largest deviation is observed when RH is taken as the

301 evaluated factor, then followed by SO_4^{2-} and NO_3^- (NO_3^- and SO_4^{2-} in autumn), which means that the

302 RH affect ALWC most and SO_4^{2-} and NO_3^- are major hygroscopic components in the aerosol. SO_4^{2-}

303 is the most influential factor for H_{air}^+, and RH, NO_3^-, and NH_3 are also important factors affecting

304 H_{air}^+. Synthetically, SO_4^{2-} and RH are two crucial factors affecting aerosol pH. For spring, winter

305 and autumn, the effect of SO_4^{2-} on aerosol pH is greater than the RH, and it is comparable with RH

306 in summer. Figure 4-6 and S2-S7 show how these factors affecting the aerosol acidity, ALWC and

307 H_{air}^+ in detail over four seasons. The sensitivity analysis for ALWC and H_{air}^+ are similar over four

308 seasons, while the sensitivity analysis of RH on aerosol pH in summer is different from the other

309 three seasons. In this study, the sensitivity analysis in winter and summer are chosen for detailed

310 description since winter is of a lot of concern due to the poor air quality while the photochemical

311 reactions are strongest in summer.

312             **Table 2**

313  The positive linear relationships between SO_4^{2-}, NO_3^-, HNO_3 concentration and ALWC as well

314 as negative linear relationship between Ca^{2+} concentration and ALWC are observed in the sensitive

315 analysis. Exponential relationships between RH and ALWC are observed, and the ALWC increased

316 rapidly with increasing RH, especially when the RH higher than 80%. Elevated NH_4^+ and NH_3

317 concentration could increase ALWC slightly. As for temperature, ALWC decreased with the

318 increasing temperature nonlinearly. High temperature could affect gas-aerosol portioning, shifts the

319 equilibrium from NO_3^- to HNO_3, underpredicted the NO_3^- and NH_4^+ concentration, thus decreasing

320   the ALWC. In addition, the higher temperature could also decrease RH and results in low ALWC in

321   the real atmosphere.

322   **Figure 5**

323   As mentioned above, SO_4^{2-} and RH are the most important factors on H_{air}^+. An exponential

324   growth of H_{air}^+ with elevated SO_4^{2-}, RH, NO_3^-, and T are found, whereas an exponential decrease

325   of H_{air}^+ with elevated NH_3 and NH_4^+ are found. Though H_{air}^+ concentration decreased linearly with

326   the augment of Ca^{2+} concentration, Ca^{2+} concentration is generally lower than 3 μg m^{-3} and generates

327   a little variation in H_{air}^+ compared to other factors. It should be noted that a "U" shape between NO_3^-

328   and H_{air}^+ are found in spring (Fig.S2), H_{air}^+ drops with the increasing NO_3^- concentration within ~20

329   μg m^{-3} and then starts to grow with the increasing NO_3^- concentration. The addition of NH_3 or NH_4^+

330   has a much more obvious effect on H_{air}^+ than ALWC. The higher the NH_3 concentration in the

331   atmosphere, the more NH_3 will dissolve in the aerosol liquid water and balance the H_{air}^+ partially.

332   Increasing temperature or RH alone will increase H_{air}^+ when other influencing factors were fixed,

333   which is consistent over four seasons.

334   **Figure 6**

335   The effects of all these factors on aerosol pH is actually a superposition of the effects on ALWC

336   and H_{air}^+. Synthetically, the effect of chemical components (NO_3^-, SO_4^{2-}, NH_4^+, Ca^{2+}) and precursor

337   gases (NH_3, HNO_3), as well as meteorological parameters (RH, T) on aerosol pH is shown in Figure

338   7. The most important influencing factor on aerosol acidity is SO_4^{2-}. The aerosol pH decreases about

339   2.8 (5 to 2.2), 6.0 (6 to 0), 1.0 (3.8 to 2.8), and 1.1 (4 to 2.9) unit with SO_4^{2-} concentration goes up

340   from 0 to 40 μg m^{-3} in spring, winter, summer, and autumn, respectively. In spring and winter, the

341   ALWC is low, the variation of SO_4^{2-} concentration could generate dramatic changes in aerosol pH.

342   In section 3.1, the aerosol pH shows an obvious seasonal variation, the aerosol pH is generally low

343   in summer whereas highest in winter, which is consistent with the SO_4^{2-} mass faction in total ions.

344   The SO_4^{2-} mass faction in total ions in summer is highest among four seasons with 32.4%±11.1%,

345   whereas it is lowest in winter with 20.9%±4.4%. Similarly, the low aerosol pH on clean days in

346   winter also relates to the leading position of SO_4^{2-} (Table 1).

347   The second important factor on aerosol acidity is RH. In the North China Plain, the severe haze

348   episodes usually occur with very high RH at a stable whether condition, resulting in the considerable

349   ALWC. In this work, except for summer, the increasing RH could reduce the aerosol pH

350   significantly when RH lower than ~30%, and then the aerosol pH decreases slowly or keeps almost

351   a constant at ~4 when the RH is between 30~80%, and the aerosol pH starts to increase with the

352   further increasing RH. However, the aerosol pH increases continuously ~1.5 unit (2.5 to 4) when

353   RH goes up from 20% to 96% in summer. The $PM_{2.5}$ concentration is lowest in summer, while the

354   RH is relatively high, the high ALWC tends to dilute H_{air}^+ and increase aerosol pH. The sensitivity

355   analysis suggests that ALWC has a different effect on aerosol pH in different seasons, the dilution

356   effect of ALWC on H_{air}^+ is obvious only in summer.

357   **Figure 7**

358   Different from SO_4^{2-}, the effect of NO_3^- on aerosol pH is not always same. In winter, summer and

359   autumn, the aerosol pH increases first and then starts to decrease when NO_3^- concentration is larger

360   than ~30 μg m^{-3}. There seems to be a threshold for the effect of NO_3^- on aerosol acidity. From a

361   mathematical point of view, the H_{air}^+ concentration increased exponentially with elevated NO_3^-

362   concentration, especially at higher NO_3^- concentrations, whereas the ALWC increase linearly with

363   elevated NO_3^- concentration. When NO_3^- concentration is less than the threshold, ALWC plays a

364   dominant role, while when the NO_3^- concentration is greater than the threshold, the H_{air}^+ has a

365   greater effect and the aerosol acidity begins to increase.

366   Moreover, in spring, the aerosol pH increases continuously with the addition of NO_3^-, which is

367   not consistent with the previous thought that addition of anion could reduce the aerosol pH. Same

368   results are found in Guo et al. (2017): at a constant ALWC, more NO_3^- is measured at higher pH.

369   Based on the measured $NO_3^-/2SO_4^{2-}$ ratio (mole mole^{-1}) of this work, we find that aerosol pH is

370   generally between 3~5 when the aerosol anionic composition is dominated by nitrate

371   ($NO_3^-/2SO_4^{2-}>1$), whereas when $NO_3^-/2SO_4^{2-}<1$, about 86% of aerosol pH is lower than 4 (Figure

372   8). In recent years, the average annual concentration of SO_4^{2-} in Beijing decreased significantly due

373   to the strict emission control measures for industries and power plants, in most cases NO_3^-

374   dominates inorganic ions (Zhao et al., 2017; Huang et al., 2017; Ma et al., 2017), which may be

375   another reason responsible for the moderately acidic aerosol.

376   Elevated NH_3 and NH_4^+ could reduce aerosol acidity by decreasing H_{air}^+ concentration

377   exponentially. In this work, NH_3 is rich in spring (21.5±8.7 µg m^{-3}), summer (19.6±6.4 µg m^{-3}) and

378   autumn (16.8±8.0 µg m^{-3}), and poor in winter (4.9±2.8 µg m^{-3}). The ratio of [TA]/2[TS] provides

379   qualitative description for the ammonia abundance, where [TA] and [TS] are the total (gas + aqueous

380   + solid) molar concentrations of ammonia and sulfate. The rich-ammonia is defined as [TA] > 2[TS],

381   while if the [TA] < 2[TS], then it is defined as poor-ammonia (Seinfeld and Pandis, 2016). In this

382   work, the ratio of [TA]/2[TS] is much higher than 1 and belongs to rich-ammonia (Fig. S8). In the

383   poor-ammonia case, there is insufficient NH_3 to neutralize the available sulfate, hence the aerosol

384   will be acidic. Whereas in the rich-ammonia case there is excess ammonia, the remaining ammonia

385   after reaction with sulfuric acid will be available to react with nitric acid to produce NH_4NO_3, so

386   that the aerosol phase will be neutralized to a large extent. However, the moderate aerosol acidity

387   suggests that though there is excess ammonia in the atmosphere, due to the limited ALWC compared

388   with the cloud liquid water content and precipitation, in most cases the aerosol will not be alkaline.

389   Furthermore, elevated Ca^{2+} concentration could increase the aerosol pH and the change of HNO_3

390   concentration has little effect on pH. Elevated temperature in favor of enhancement the aerosol

391   acidity by reducing ALWC and increasing H_{air}^+.

392   **Figure 8**

393   **3.4 Size distribution of aerosol components and pH**

394   According to the average $PM_{2.5}$ concentration during every sampling period, all the samples are

395   also classified into three groups (clean, polluted, heavily polluted) with the same rule described in

396   Section 3.2. A severe haze episode occurred during the autumn sampling, hence there were more

397   heavily polluted samples for autumn than that in other seasons. Figure 9 shows the averaged size

398   distributions of PM components and pH on clean, polluted and heavily polluted days in summer,

399   autumn and winter, respectively. The NO_3^-, SO_4^{2-}, NH_4^+, Cl^-, K^+, OC, and EC were mainly

400   concentrated in the size range with aerodynamic diameters between 0.32~3.1µm, while Mg^{2+} and

401   Ca^{2+} were predominantly distributed in the coarse mode. As shown in Figure 9, the concentration

402   levels for all chemical components increased with the increasing pollution. During the haze episodes,

403   the sulfate and nitrate in the accumulated mode increased significantly. However, the increase of

404   Mg^{2+} and Ca^{2+} in the coarse mode were not as obvious as secondary ions, mainly due to the low

405   wind speed and calm atmosphere which make it more difficult to raise dust during the heavy

406   pollution. More detailed information about size distributions of mass concentration for all analyzed

407   species during three seasons is shown in Zhao et al. (2017) and Su et al. (2018).

408   **Figure 9**

409   The aerosol pH for both accumulation mode and coarse mode in summer were lowest among

410   three seasons, then followed by autumn and winter. In summer, the predominance of sulfate in the

411   fine mode resulted in a low pH, ranging between 1.8 and 3.9. The sensitivity analysis of this work

412   shows sulfate plays a key role in predicting pH, its high hygroscopicity leads to the formation of the

413   aqueous drops and provides H_{air}^+ (Fang et al., 2017). Aerosol pH for fine particles in autumn and

414   winter are in the range of 2.4 ~ 6.3 and 3.5 ~ 6.5, respectively. As for coarse particles, the predicted

415   pH is approximately near or even higher than 7 for all of the three seasons in this work. It should be

416   noted that assuming coarse mode particles in equilibrium with the gas phase generally overestimates

417   acidity (pH<4) (Fang et al., 2017).

418   On heavily polluted days, the aerosol pH in coarse mode showed a marked fall in autumn and

419   winter. For example, the pH in stage 3 (3.1-6.2 μm) declined from 7.8 on clean days to 4.5 on heavily

420   polluted days in winter, implying that the aerosols in coarse mode during severe hazy days would

421   become weak acid from neutral. The obvious increase of nitrate in coarse mode may responsible for

422   this. Moreover, the significant decrease of mass ratios of Ca^{2+} and Mg^{2+} also weakened the alkaline.

423   The size distribution of aerosol pH and all analyzed chemical components in the daytime and

424   nighttime are illustrated in Figure 10. For summer and autumn, the pH in the nighttime is higher

425   than that in the daytime. Whereas, in winter, the pH is higher in the daytime. The diurnal variation

426   for aerosol pH based on MOUDI data is consistent with the online data. In the daytime of summer

427   and autumn, the solar radiation is strong and photochemical reaction is active as well as the RH is

428   lower, leading to a lower aerosol pH than nighttime. In winter, the averaged RH during the sampling

429   period is 43%, leading to a low ALWC, but the SO_4^{2-} and NO_3^- in the nighttime are obviously higher

430   due to the lower boundary layer. Therefore, H_{air}^+ is more abundant in nighttime while the low ALWC

431 had little effect on pH.

432 **Figure 10**

433 **5. Summary and conclusions**

434   Aerosol acidity is important for the formation of secondary aerosol and is of many challenges to

435 be measured directly. In this work, ISORROPIA-II with forward mode is applied to calculate the

436 H_{air}^+ and ALWC based on the 1-h $PM_{2.5}$ inorganic ions, precursor gases (HCl, HNO_3, NH_3) and RH,

437 T. Moreover, the size distribution of pH is predicted based on the MOUDI samples with the same

438 way, the gas-phase NH_3, HNO_3 and HCl are determined through an iteration procedure. In Beijing,

439 the mean aerosol pH over four seasons is 4.3±1.6 (spring), 4.5±1.1(winter), 3.9±1.3(summer),

440 4.1±1.0 (autumn), respectively, showing the moderate aerosol acidity. The seasonal variation of

441 aerosol pH is closely related to the SO_4^{2-}. Overall, the aerosol is more acidic on hazy days than clean

442 days. The aerosol pH in fine mode is in the range of 1.8 ~ 3.9, 2.4 ~ 6.3 and 3.5 ~ 6.5 for summer,

443 autumn and winter, respectively. As for coarse particles, the predicted pH is approximately near or

444 even higher than 7.

445   Due to the significantly high level of hygroscopic components in particulate matter in Beijing,

446 pH has a diurnal trend that follows both aerosol components (especially the sulfate) and ALWC. For

447 spring, summer and autumn, the averaged nighttime pH is 0.3~0.4 unit higher than that on daytime.

448 However, in winter, H_{air}^+ in nighttime is slightly higher than that in daytime and the aerosol pH is

449 relatively low at night and higher at sunset. This result is very different from that found in

450 southeastern United States: the pH diurnal variation is largely driven by meteorological conditions.

451   A sensitivity analysis is performed in this work to investigate how aerosol components, precursor

452 gases and meteorological conditions affect aerosol acidity. The RH affects ALWC most, then

453 followed by SO_4^{2-} and NO_3^-. For H_{air}^+, SO_4^{2-} is the most influential factor, and RH, NO_3^-, NH_3 are

454 also important factors affecting H_{air}^+. Synthetically, SO_4^{2-} and RH are two crucial factors affecting

455 aerosol pH. For spring, winter and autumn, the effect of SO_4^{2-} on aerosol pH is greater than RH, and

456 it is comparable with RH in summer. The aerosol pH decreases with elevated SO_4^{2-} concentration,

457 the variation of SO_4^{2-} concentration could generate dramatic changes in aerosol pH in spring and

458 winter. As the NO_3^- concentration increases, the aerosol pH firstly increases and then decrease at a

459   inflection point with 30 μg m^{-3}. In this work, sulfate-dominant aerosols are more acidic with pH

460   lower than 4, whereas nitrate-dominated aerosols are weak in acidity with pH ranges 3~5. In recent

461   years, the SO_4^{2-} concentration of $PM_{2.5}$ in Beijing decreased significantly due to the strict emission

462   control measures, in most cases NO_3^- dominates inorganic ions, which may be another reason

463   responsible for the moderately acidic aerosol.

464   ALWC has a different effect on aerosol pH in different seasons. In winter, the increasing RH

465   could reduce the aerosol pH whereas it shows a totally reverse tendency in summer, and the elevated

466   RH has little effect on aerosol pH in spring and autumn when the RH is between 30% and 80%. The

467   sensitivity analysis of this work highlights the diverse influence of ALWC on aerosol pH, the

468   dilution effect of ALWC on H_{air}^+ is only obvious in summer. The elevated NH_3 and NH_4^+ could

469   reduce aerosol acidity by decreasing H_{air}^+ concentration exponentially. In the North China Plain, the

470   ammonia is rich, the remaining ammonia after reaction with sulfuric acid will be available to react

471   with nitric acid to produce NH_4NO_3, so that the aerosol phase will be neutralized to a large extent.

472   However, the moderate aerosol acidity suggests that though there are excess ammonia in the

473   atmosphere, in most cases the aerosol will not be alkaline due to the limited ALWC.

474

475   **Acknowledgments**

476   This work was supported by the National Natural Science Foundation of China (41675131),

477   the Beijing Talents Fund (2014000021223ZK49), the Beijing Natural Science Foundation

478   (8131003).

479   **References**

480   Bian, Y. X., Zhao, C. S., Ma, N., Chen, J., Xu, W. Y.: A study of aerosol liquid water content based

481   on hygroscopicity measurements at high relative humidity in the North China Plain. Atmos. Chem.

482   Phys. 14, 6417-6426, 2014.

483   Bougiatioti, A., Nikolaou, P., Stavroulas, I., Kouvarakis, G., Weber, R., Nenes, A., Kanakidou, M.,

484   Mihalopoulos, N.: Particle water and pH in the eastern Mediterranean: Source variability and

485   implications for nutrient availability, Atmos. Chem. Phys., 16(7), 4579-4591, 2016.

486   Cheng, Y. F., Zheng, G. J., Wei C., Mu, Q., Zheng, B., Wang, Z. B., Gao, M., Zhang, Q., He, K. B.,

487   Carmichael, G., Pöschl, U., Su, H.: Reactive nitrogen chemistry in aerosol water as a source of

488   sulfate during haze events in China, Sci. Adv., 2:e1601530, 2016.

489   Clegg, S. L., et al.: A thermodynamic model of the system H^+, NH_4^+, SO_4^{2-}, NO_3^-, H_2O at

490   tropospheric temperatures, J. Phys. Chem. 102A, 2137-2154, 1998.

491   Covert, D.S., Charlson, R.J., Ahlquist, N.C.: A study of the relationship of chemical composition

492   and humidity to light scattering by aerosol. J. Appl. Meteorol. 11, 968-976, 1972.

493   Cruz, C. N., Dassios, K. G., Pandis, S. N.: The effect of dioctyl phthalate films on the ammonium

494   nitrate aerosol evaporation rate. Atmos. Environ., 34, 3897-3905, 2000.

495   Dassios, K. G., Pandis, S. N.: The mass accommodation coefficient of ammonium nitrate aerosol.

496   Atmos. Environ., 33 (18), 2993-3003, 1999.

497   Eddingsaas, N. C., VanderVelde, D. G., and Wennberg, P. O.: Kinetics and products of the acid-

498   catalyzed ring-opening of atmospherically relevant butyl epoxy alcohols, J. Phys. Chem. A, 114,

499   8106-8113, 2010.

500   Fang, T., Guo, H. Y., Zeng, L. H., Verma, V., Nenes, A., Weber, R. J.: Highly acidic ambient particles,

501   soluble metals, and oxidative potential: A link between sulfate and aerosol toxicity, Environ. Sci.

502   Technol., 51, 2611-2620, 2017.

503   Fountoukis, C., and Nenes, A.: ISORROPIA II A computationally efficient aerosol thermodynamic

504   equilibrium model for K^+, Ca^{2+}, Mg^{2+}, NH_4^+, Na^+, SO_4^{2-}, NO_3^-, Cl^-, H_2O aerosols, Atmos. Chem.

505   Phys. 7, 4639-4659, 2007.

506   Fountoukis, C., Nenes, A., Sullivan, A., Weber, R., Van Reken, T., Fischer, M., Matías, E., Moya,

507   M., Farmer, D., and Cohen, R. C.: Thermodynamic characterization of Mexico City aerosol

508   during MILAGRO 2006, Atmos. Chem. Phys., 9, 2141-2156, 2009.

509   Gao, J. J., Wang, K., Wang, Y., Liu, S. H., Zhu, C. Y., Hao, J. M., Liu, H. J., Hua, S. B., Tian, H. Z.:

510   Temporal-spatial characteristics and source apportionment of $PM_{2.5}$ as well as its associated

511   chemical species in the Beijing-Tianjin-Hebei region of China. Environ. Pollut., 233, 714-724,

512   2018.

513   Guo, H., Sullivan, A. P., Campuzano-Jost, P., Schroder, J. C., Lopez-Hilfiker, F. D., Dibb, J. E.,

514   Jimenez, J. L., Thornton, J. A., Brown, S. S., Nenes, A., Weber, R. J.: Fine particle pH and the

515   partitioning of nitric acid during winter in the northeastern United States, J. Geophys. Res. Atmos.,

516   121, 10355-10376, 2016.

517   Guo, H., Xu, L., Bougiatioti, A., Cerully, K. M., Capps, S. L., Hite Jr., J. R., Carlton, A. G., Lee, S.-

518   H., Bergin, M. H., Ng, N. L., Nenes, A., Weber, R. J.: Fine-particle water and pH in the

519   southeastern United States, Atmos. Chem. Phys., 15, 5211-5228, 2015.

520   Guo, S., Hu, M., Zamor, M. L., Peng, J. F., Shang, D. J., Zheng, J., Du, Z. F., Wu, Z. J., Shao, M.,

521   Zeng, L. M., Molinac, M. J., Zhang R. Y.: Elucidating severe urban haze formation in China.

522   PNAS, 111(49): 17373-17378, 2014.

523   Hennigan, C. J., Izumi, J., Sullivan, A. P., Weber, R. J., and Nenes, A.: A critical evaluation of proxy

524   methods used to estimate the acidity of atmospheric particles, Atmos. Chem. Phys., 15, 2775-

525   2790, 2015.

526   Huang, X. J., Liu, Z. R., Liu, J. Y., Hu, B., Wen, T. X., Tang, G. Q., Zhang, J. K., Wu, F. K., Ji, D.

527   S., Wang, L. L., Wang, Y. S.: Chemical characterization and source identification of $PM_{2.5}$ at

528   multiple sites in the Beijing–Tianjin–Hebei region, China, Atmos. Chem. Phys., 17, 12941–12962,

529   2017.

530   Jang, M., Czoschke, N. M., Lee, S., and Kamens, R. M.: Heterogeneous atmospheric aerosol

531   production by acidcatalyzed particle-phase reactions, Science, 298, 814-817, 2002.

532   Kuang, Y., Zhao, C. S., Ma, N., Liu, H. J., Bian, Y. X., Tao, J. C., and Hu, M.: Deliquescent

533   phenomena of ambient aerosols on the North China Plain. Geophys. Res. Lett., 43, doi:

534   10.1002/2016GL070273, 2016.

535   Kuang, Y., Zhao, C. S., Zhao, G., Tao, J. C., Ma, N., and Bian, Y. X.: A novel method for calculating

536   ambient aerosol liquid water contents based on measurements of a humidified nephelometer

537   system. Atmos. Meas. Tech. Discuss., doi.org/10.5194/amt-2017-330, 2017a.

538   Kuang, Y., Zhao, C. S., Tao, J. C., Bian, Y. X., Ma, N., and Zhao, G.: A novel method for deriving

539   the aerosol hygroscopicity parameter based only on measurements from a humidified

540   nephelometer system. Atmos. Chem. Phys., 17, 6651–6662, 2017b.

541   Liu, B. Y. H., Pui, D. Y. H., Whitby, K. T., et al.: The aerosol mobility chromatograph - new detector

542   for sulfuric-acid aerosols. Atmos. Environ., 12(1-3), 99-104, 1978.

543   Liu, P. F., Zhao, C. S., Göbel, T., Hallbauer, E., Nowak, A., Ran, L., Xu, W. Y., Deng, Z. Z., Ma, N.,

544   Mildenberger, K., Henning, S., Stratmann, F., and Wiedensohler, A.: Hygroscopic properties of

545   aerosol particles at high relative humidity and their diurnal variations in the North China Plain,

546   Atmos. Chem. Phys., 11, 3479-3494, 2011.

547   Liu, H. J., Zhao, C. S., Nekat, B., et al.: Aerosol hygroscopicity derived from size-segregated

548   chemical composition and its parameterization in the North China Plain. Atmos. Chem. Phys.,

549   14 :2525-2539, 2014.

550   Liu, Z., Wu, L. Y., Wang, T. H., et al.: Uptake of methacrolein into aqueous solutions of sulfuric

551   acid and hydrogen peroxide. J. Phys. Chem. A, 116, 437-442, 2012.

552   Ma, Q.X., Wu, Y.F., Zhang, D. Z., Wang, X.J., Xia, Y.J., Liu, X.Y., Tian, P., Han, Z.W., Xia, X.G.,

553   Wang, Y., Zhang, R.J.: Roles of regional transport and heterogeneous reactions in the $PM_{2.5}$

554   increase during winter haze episodes in Beijing, Sci. Total Environ., 599-600, 246-253, 2017.

555   Meskhidze, N., Chameides, W. L., Nenes, A., and Chen, G.: Iron mobilization in mineral dust: Can

556   anthropogenic SO_2 emissions affect ocean productivity? Geophys. Res. Lett., 30, 2085,

557   doi:10.1029/2003gl018035, 2003.

558   Nenes, A., et al.: ISORROPIA: A new thermodynamic model for multiphase multicomponent

559   inorganic aerosols, Aquatic Geochem. 4, 123-152, 1998.

560   Nowak, J. B., Huey, L. G., Russell, A. G., Tian, D., Neuman, J. A., Orsini, D., Sjostedt, S. J., Sullivan,

561   A. P., Tanner, D. J., Weber, R. J., Nenes, A., Edgerton, E., Fehsenfeld, F. C.: Analysis of urban

562   gas phase ammonia measurements from the 2002 Atlanta Aerosol Nucleation and Real-Time

563   Characterization   Experiment   (ANARChE),   J.   Geophys.   Res.,   111,   D17308,

564   doi:10.1029/2006jd007113, 2006.

565   Pathak, R. K., Wang, T., Ho, K. F., Lee, S. C.: Characteristics of summertime $PM_{2.5}$ organic and

566   elemental carbon in four major Chinese cities: Implications of high acidity for water soluble

567   organic carbon (WSOC), Atmos. Environ., 45, 318-325, 2011a.

568   Pathak, R. K., Wang, T. and Wu, W.S.: Nighttime enhancement of $PM_{2.5}$ nitrate in ammonia-poor

569   atmospheric conditions in Beijing and Shanghai: Plausible contributions of heterogeneous

570   hydrolysis of N_2O_5 and HNO_3 partitioning. Atmos. Environ., 45: 1183-1191, 2011b.

571   Peng, C. G., Chan, M. N., and Chan, C. K.: The hygroscopic properties of dicarboxylic and

572   multifunctional acids: Measurements and UNIFAC predictions, Environ. Sci. Technol. 35, 4495-

573   4501, 2001.

574   Pye, H. O., Pinder, R. W., Piletic, I. R., Xie, Y., Capps, S. L., Lin, Y. H., Surratt, J. D., Zhang, Z.,

575   Gold, A., Luecken, D. J., Hutzell, W. T., Jaoui, M., Offenberg, J. H., Kleindienst, T. E.,

576   Lewandowski, M., and Edney, E. O.: Epoxide pathways improve model predictions of isoprene

577   markers and reveal key role of acidity in aerosol formation, Environ. Sci. Technol., 47, 11056-

578   11064, 2013.

579   Rengarajan, R., Sudheer, A.K., Sarin, M.M.: Aerosol acidity and secondary formation during

580   wintertime over urban environment in western India. Atmos. Environ., 45: 1940-1945, 2011.

581   Rood, M.J., Larson, T.V., Covert, D.S., Ahlquist, N.C.: Measurement of laboratory and ambient

582   aerosols with temperature and humidity controlled nephelometry. Atmos. Environ. 19, 1181-1190,

583   1985.

584   Schwertmann, U., Cornell, R. M.: Iron Oxides In the Laboratory: Preparation and Characterization,

585   Weinheim, WCH Publisher, 1991.

586   Seinfeld, J. H., Pandis, S. N.: Atmospheric Chemistry and Physics: From Air Pollution to Climate

587   Change, John Wiley & Sons, Inc., Hoboken, New Jersey, USA, 2016.

588   Shi, G. L., Xu, J., Peng, X., Xiao, Z. M., Chen, K., Tian, Y. Z., Guan, X. P., Feng, Y. C., Yu, H. F.,

589   Nenes, A., Russell, A. G.: pH of aerosols in a polluted atmosphere: source contributions to highly

590   acidic aerosol, Environ. Sci. Technol., DOI: 10.1021/acs.est.6b05736, 2017.

591   Shi, Z., Bonneville, S., Krom, M. D., Carslaw, K. S., Jickells, T. D., Baker, A. R., Benning, L. G.:

592   Iron dissolution kinetics of mineral dust at low pH during simulated atmospheric processing.

593   Atmos. Chem. Phys., 11, 995-1007, 2011.

594   Song, S. J., Gao, M., Xu, W. Q., Shao, J. Y., Shi, G. L., Wang, S. X., Wang, Y. X., Sun, Y. L., McElroy,

595   M. B.: Fine particle pH for Beijing winter haze as inferred from different thermodynamic

596   equilibrium models. Atmos. Chem. Phys. Discuss., doi.org/10.5194/acp-2018-6, 2018.

597   Su, J., Zhao, P. S., Dong, Q.: Chemical Compositions and Liquid Water Content of Size-Resolved

598   Aerosol in Beijing. Aerosol Air Qual. Res., 18, 680-692, 2018.

599   Surratt, J. D., Chan, A. W., Eddingsaas, N. C., Chan, M., Loza, C. L., Kwan, A. J., Hersey, S. P.,

600   Flagan, R. C., Wennberg, P. O., and Seinfeld, J. H.: Reactive intermediates revealed in secondary

601   organic aerosol formation from isoprene, P. Natl. Acad. Sci. USA, 107, 6640-6645, 2010.

602   Swietlicki, E., Hansson, H.-C., Hämeri, K., Svenningsson, B., Massling, A., McFiggans, G.,

603   McMurry, P.H., Petäjä, T., Tunved, P., Gysel, M., Topping, D., Weingartner, E., Baltensperger, U.,

604   Rissler, J., Wiedensohler, A., Kulmala, M.: Hygroscopic properties of submicrometer

605   atmospheric aerosol particles measured with H-TDMA instruments in various environments: a

606   review. Tellus Ser. B Chem. Phys. Meteorol. 60, 432-469, 2008.

607   Tan, T. Y., Hu, M., Li, M. R., Guo, Q. F., Wu, Y. S., Fang, X., Gu, F. T., Wang, Y., Wu, Z. J.: New

608   insight into $PM_{2.5}$ pollution patterns in Beijing based on one-year measurement of chemical

609   compositions. Sci. Total Environ., 621, 734-743, 2018.

610   ten Brink, H., Otjes, R., Jongejan, P., Slanina, S.: An instrument for semicontinuous monitoring of

611   the size-distribution of nitrate, ammonium, sulphate and chloride in aerosol. Atmos. Environ. 41,

612   2768-2779, 2007.

613   Topping, D. O., McFiggans, G. B., and Coe, H.: A curved multicomponent aerosol hygroscopicity

614   model framework: Part 1– Inorganic compounds, Atmos. Chem. Phys., 5, 1205-1222, 2005a.

615   Topping, D. O., McFiggans, G. B., and Coe, H.: A curved multicomponent aerosol hygroscopicity

616   model framework: Part 2 – Including organic compounds, Atmos. Chem. Phys., 5, 1223-1242,

617   2005b

618   Wang, G., Zhang, R., Gomez, M. E., Yang, L., Levy Zamora, M., Hu, M., Lin, Y., Peng, J., Guo, S.,

619   Meng, J., Li, J., Cheng, C., Hu, T., Ren, Y., Wang, Y., Gao, J., Cao, J., An, Z., Zhou, W., Li, G.,

620   Wang, J., Tian, P., Marrero-Ortiz, W., Secrest, J., Du, Z., Zheng, J., Shang, D., Zeng, L., Shao,

621   M., Wang, W., Huang, Y., Wang, Y., Zhu, Y., Li, Y., Hu, J., Pan, B., Cai, L., Cheng, Y., Ji, Y.,

622   Zhang, F., Rosenfeld, D., Liss, P. S., Duce, R. A., Kolb, C. E., and Molina, M. J.: Persistent sulfate

623   formation from London Fog to Chinese haze, Proc. Natl. Acad. Sci. U.S.A., 113, 13630-13635,

624   2016.

625   Wang, X. W., Jing, B., Tan, F., Ma, J.B., Zhang, Y. H., Ge, M.F.: Hygroscopic behavior and chemical

626   composition evolution of internally mixed aerosols composed of oxalic acid and ammonium

627   sulfate, Atmos. Chem. Phys., 17, 12797-12812, 2017.

628   Weber, R. J., Guo, H., Russell, A. G., Nenes, A.: High aerosol acidity despite declining atmospheric

629   sulfate concentrations over the past 15 years. Nat. Geosci., 9, 282-285, 2016.

630   Yan, P., Pan, X., Tang, J., et al.: Hygroscopic growth of aerosol scattering coefficient: A comparative

631   analysis between urban and suburban sites at winter in Beijing. Particuology, 7, 52-60, 2009.

632   Young, A. H., Keene, W. C., Pszenny, A. A. P., Sander, R., Thornton, J. A., Riedel, T. P., Maben, J.

633   R.: Phase partitioning of soluble trace gases with size-resolved aerosols in near-surface

634   continental air over northern Colorado, USA, during winter, J. Geophys. Res. Atmos., 118, 9414-

635   9427, doi:10.1002/jgrd.50655, 2013.

636   Zhang, Q., Jimenez, J. L., Worsnop, D. R., Canagaratna, M.: A case study of urban particle acidity

637   and its influence on secondary organic aerosol. Environ. Sci. Technol., 41, 3213-3219, 2007.

638   Zhao, P. S., Chen, Y. N., Su, J.: Size-resolved carbonaceous components and water-soluble ions

639   measurements of ambient aerosol in Beijing. J. Environ. Sci., 54, 298-313, 2017.

640   Zhao, P.S., Dong, F., He, D., Zhao, X.J., Zhang, X.L., Zhang, W.Z., Yao, Q., Liu, H. Y.:

641   Characteristics of concentrations and chemical compositions for $PM_{2.5}$ in the region of Beijing,

642   Tianjin, and Hebei, China. Atmos. Chem. Phys., 13, 4631-4644, 2013.

643   Zou, J. N., Liu, Z. R., Hu, B., Huang, X. J., Wen, T. X., Ji, D. S., Liu, J. Y., Yang, Y., Yao, Q., Wang,

644   Y. S.: Aerosol chemical compositions in the North China Plain and the impact on the visibility in

645   Beijing and Tianjin. Atmos. Res. 201, 235-246, 2018.

646

Table captions

647

648 **Table 1.** The averaged $PM_{2.5}$ and NO_3^-, SO_4^{2-}, NH_4^+ mass concentration as well as RH, ALWC,

649 H_{air}^+, pH on clean, polluted and heavily polluted days over four seasons.

650 **Table 2.** Sensitivity of aerosol chemical components (NO_3^-, SO_4^{2-}, NH_4^+, Ca^{2+}), precursor gases

651 (NH_3, HNO_3) and meteorological parameters (RH, T) to aerosol acidity, ALWC and H_{air}^+. The larger

652 magnitude of the deviation represents the larger impact.

653
654

655

656 **Table 1**

Spring	PM$_{2.5}$	NO$_3^-$	SO$_4^{2-}$	NH$_4^+$	ALWC	H$_{air}^+$	pH
	µg m^{-3}	µg m^{-3}	µg m^{-3}	µg m^{-3}	µg m^{-3}	µg m^{-3}	
Averaged	62±36	14.9±14.6	9.7±7.9	7.9±7.3	17±30	4.7E-06±9.5E-06	4.3±1.6
Clean	44±17	7.9±6.6	6.2±3.7	4.8±3.2	10±21	3.5E-06±8.4E-06	4.5±1.9
Polluted	100±21	30.8±14.3	16.4±5.9	15.4±5.8	28±34	5.6E-06±7.4E-06	3.9±0.7
Heavily polluted	169±12	45.3±8.5	36.3±4.9	29.4±2.3	77±60	1.9E-05±6.1E-06	3.6±0.3
winter	PM$_{2.5}$	NO$_3^-$	SO$_4^{2-}$	NH$_4^+$	ALWC	H$_{air}^+$	pH
Averaged	60±69	13.7±21.0	7.3±8.7	7.3±10.0	17±37	9.0E-06±1.3E-04	4.5±1.1
Clean	22±20	3.6±3.9	2.8±1.8	2.2±2.0	4±11	2.6E-07±4.2E-07	4.3±1.1
Polluted	107±21	18.9±8.6	11.0±5.7	11.0±4.7	31±42	1.2E-05±6.9E-05	5.3±1.2
Heavily polluted	209±39	59.7±21.8	26.2±6.3	29.1±8.7	77±51	5.2E-05±3.4E-04	4.5±0.7
Summer	PM$_{2.5}$	NO$_3^-$	SO$_4^{2-}$	NH$_4^+$	ALWC	H$_{air}^+$	pH
Averaged	39±24	9.5±9.5	8.6±7.5	7.2±5.6	51±68	1.6E-05±1.6E-05	3.9±1.3
Clean	33±18	7.3±6.8	7.0±6.0	5.9±4.0	41±61	1.3E-05±1.6E-05	3.9±1.3
Polluted	87±13	26.5±10.5	20.7±7.0	17.6±4.8	102±85	3.1E-05±1.7E-06	3.5±0.4
Autumn	PM$_{2.5}$	NO$_3^-$	SO$_4^{2-}$	NH$_4^+$	ALWC	H$_{air}^+$	pH
Averaged	59±48	18.5±19.5	6.5±5.9	8.2±8.2	91±145	1.1E-05±1.5E-05	4.1±1.0
Clean	33±21	7.6±7.4	4.4±4.1	3.8±3.5	37±72	5.1E-06±9.4E-06	4.2±1.2
Polluted	105±21	33.8±11.6	14.3±6.3	16.0±4.6	182±172	1.8E-05±1.3E-05	3.9±0.4
Heavily polluted	174±18	63.4±15.4	25.0±15.9	29.0±5.1	315±212	3.6E-05±2.6E-05	3.9±0.3

657

658

659

660

661

662

663

Table 2

Impact Factor		SO_4^{2-}	NO_3^-	NH_4^+	Ca^{2+}	RH	T	NH_3	HNO_3
Spring	D-ALWC	**3.8**	**2.0**	0.2	0.9	**14.2**	0.7	0.3	0.1
	D-H_{air}^+	**1.4E-05**	6.9E-07	2.9E-07	7.0E-07	**2.1E-06**	9.1E-07	**1.2E-06**	2.4E-08
	D-pH	**0.7**	0.4	0.2	0.3	**0.5**	0.4	0.3	0.0
Winter	D-ALWC	**3.2**	1.5	0.6	0.2	**16.6**	0.4	0.1	0.1
	D-H_{air}^+	**2.6E-04**	5.8E-07	2.5E-06	1.9E-07	5.9E-07	2.8E-07	2.5E-07	1.9E-07
	D-pH	**1.4**	0.4	0.9	0.1	**1.3**	0.4	0.2	0.0
Summer	D-ALWC	**10.0**	**9.1**	0.5	1.8	**43.9**	2.1	0.8	0.3
	D-H_{air}^+	**1.7E-05**	2.5E-06	2.0E-06	1.6E-06	5.0E-06	3.0E-06	**4.1E-06**	5.8E-08
	D-pH	**0.3**	0.1	0.1	0.1	**0.3**	0.2	**0.2**	0.0
Autumn	D-ALWC	**10.3**	**16.7**	0.2	1.1	**83.5**	2.0	0.3	0.4
	D-H_{air}^+	**1.6E-05**	**1.5E-05**	1.9E-06	4.8E-07	6.7E-06	3.0E-06	2.5E-06	4.6E-08
	D-pH	**0.3**	0.2	0.2	0.0	**0.2**	**0.3**	0.2	0.0

664

665

Figure captions

666

667 **Figure 1.** Time series of relative humidity (RH), temperature (T) (a, e, i, m); $PM_{2.5}$, PM_{10}, and NH_3

668 (b, f, g, n); dominant water-soluble ion species: NO_3^-, SO_4^{2-}, NH_4^+ (c, g, k, o); aerosol pH colored

669 by $PM_{2.5}$ concentration (d, h, l, p) over four seasons.

670 **Figure 2.** Comparisons of predicted NO_3^-, NH_4^+ to measured values based on (a, b) online ion

671 chromatography data and (c, d) MOUDI data.

672 **Figure 3.** Wind dependence map of aerosol pH over four seasons. In each picture, the shaded

673 contour indicates the average of variables for varying wind speeds (radial direction) and wind

674 directions (transverse direction).

675 **Figure 4.** Diurnal patterns of predicted aerosol liquid water content (ALWC) (a-d); H_{air}^+ predicted

676 by ISORROPIAII (i-l); predicted aerosol pH (m-p) over four seasons. Mean and median values are

677 shown, together with 25% and 75 % quantiles.

678 **Figure 5.** Sensitivities of chemical components (NO_3^-, SO_4^{2-}, NH_4^+, Ca^{2+}), precursor gases (NH_3,

679 HNO_3) as well as meteorological parameters (RH, T) to ALWC in summer and winter.

680 **Figure 6.** Sensitivities of chemical components (NO_3^-, SO_4^{2-}, NH_4^+, Ca^{2+}), precursor gases (NH_3,

681 HNO_3) as well as meteorological parameters (RH, T) to H_{air}^+ in summer and winter.

682 **Figure 7.** Sensitivities of chemical components (NO_3^-, SO_4^{2-}, NH_4^+, Ca^{2+}), precursor gases (NH_3,

683 HNO_3) as well as meteorological parameters (RH, T) to pH in summer and winter.

684 **Figure 8.** Measured $NO_3^-/2SO_4^{2-}$ ratio (mole $mole^{-1}$) versus predicted pH colored by ambient RH.

685 NO_3^-, SO_4^{2-} dominant zone denotes $NO_3^-/2SO_4^{2-} > 1$ or < 1.

686 **Figure 9.** The size distribution of aerosol pH and all analyzed chemical components on clean (a, d,

687 g), polluted (b, e, h) and heavily polluted days (c, f, i) in summer, autumn and winter.

688 **Figure 10.** The size distribution of pH and all analyzed chemical components in the daytime (a, c,

689 e) and (b, d, f) nighttime in summer, autumn and winter.

690
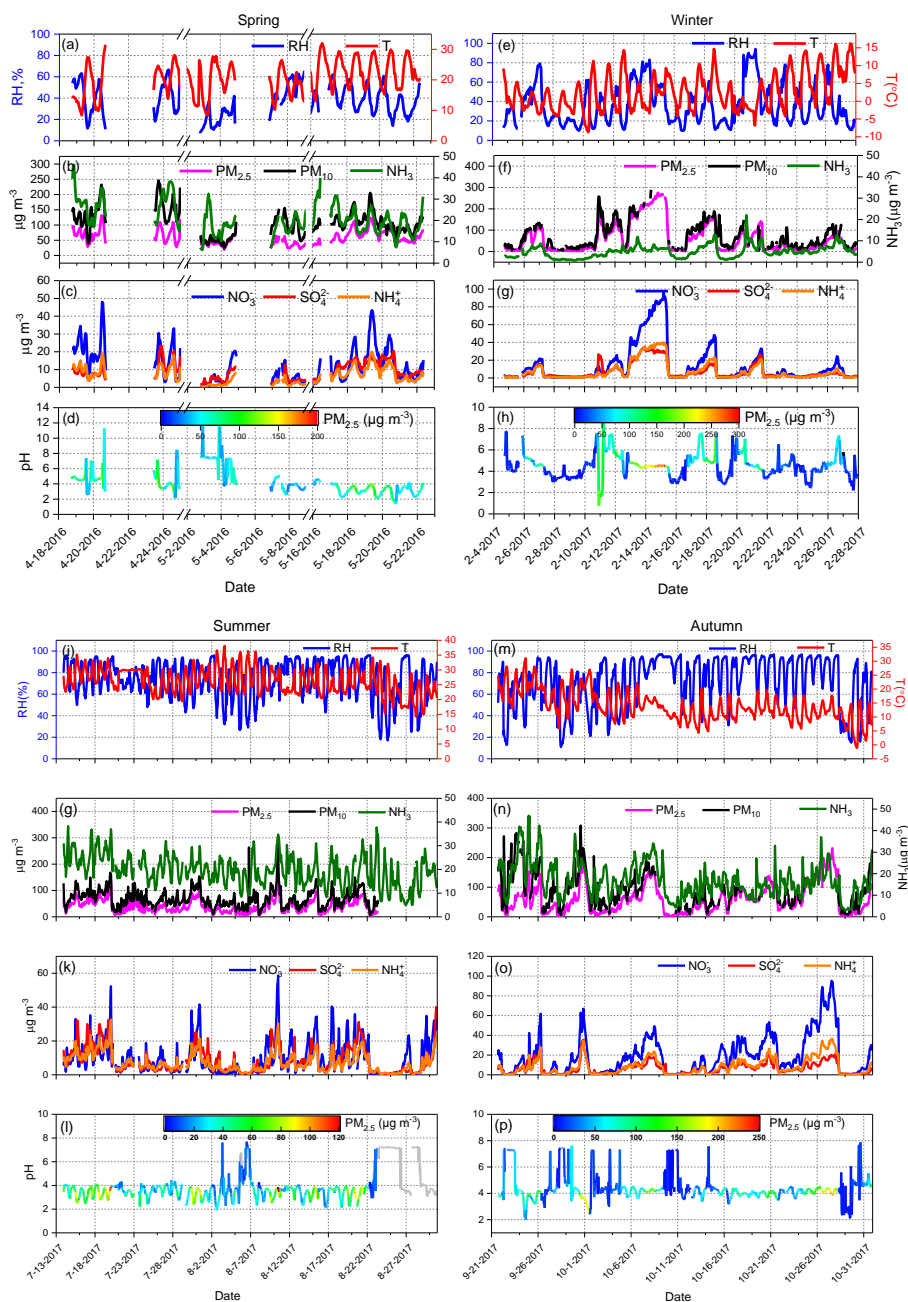
691

Figure 1.

692

693

694

695

696
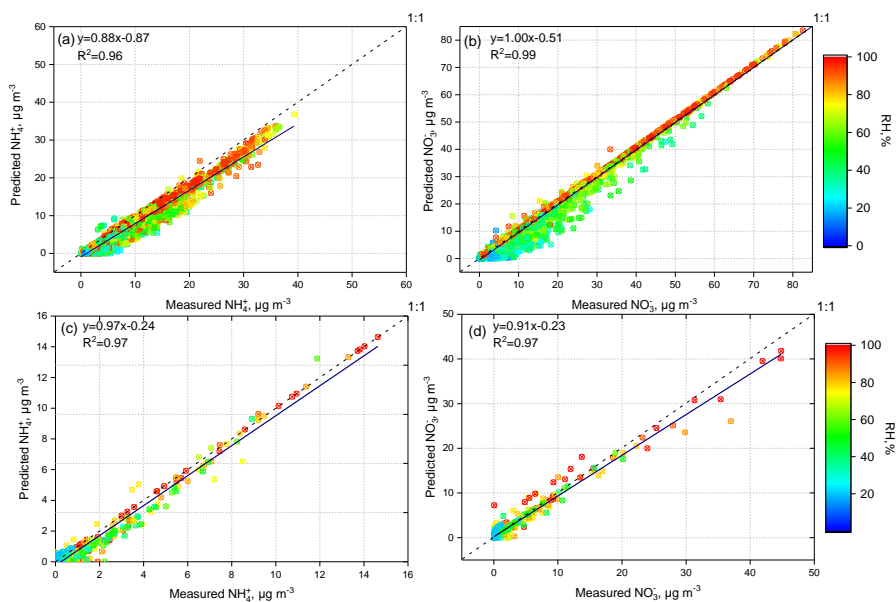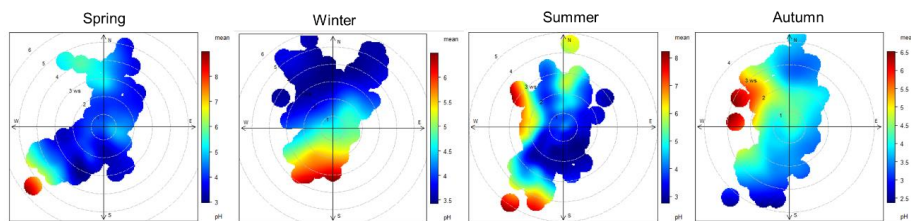
697

698   **Figure 2.**

699

700

701

702

703   **Figure 3.**

704
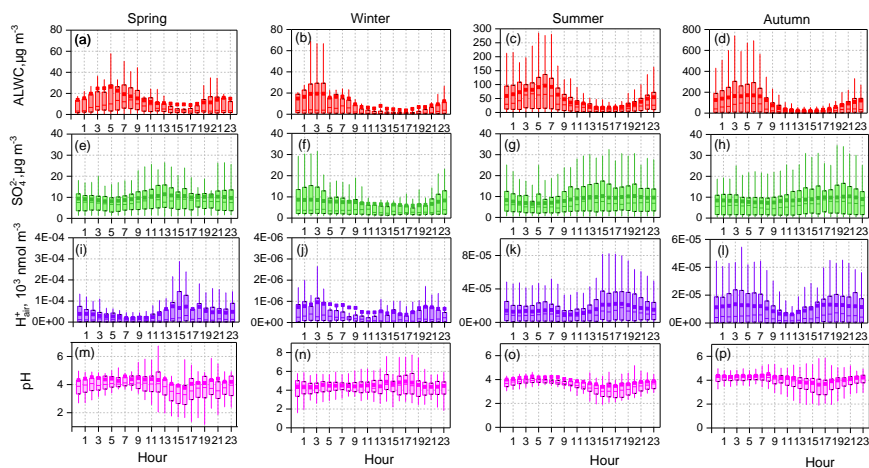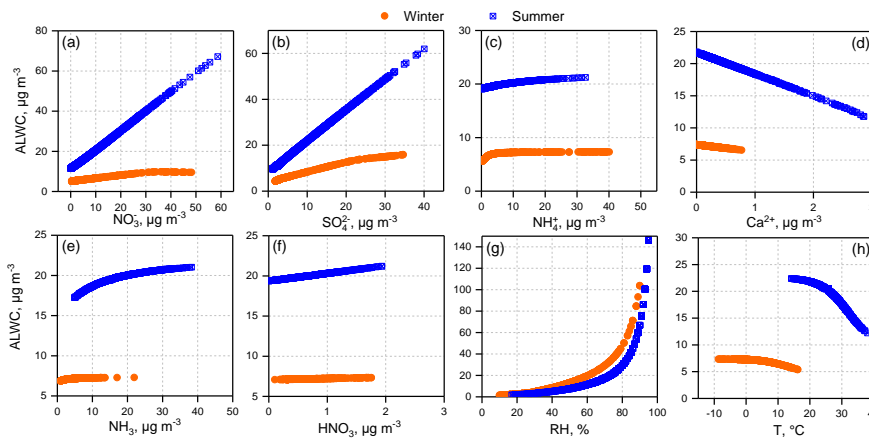
Figure 4.

Figure 5.

714

715

Figure 6.

716

717

718

Figure 7.

719

720

721   **Figure 8.**

722

723
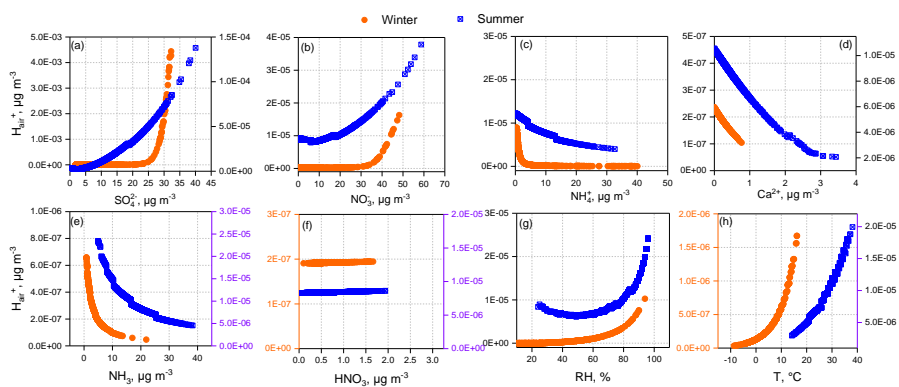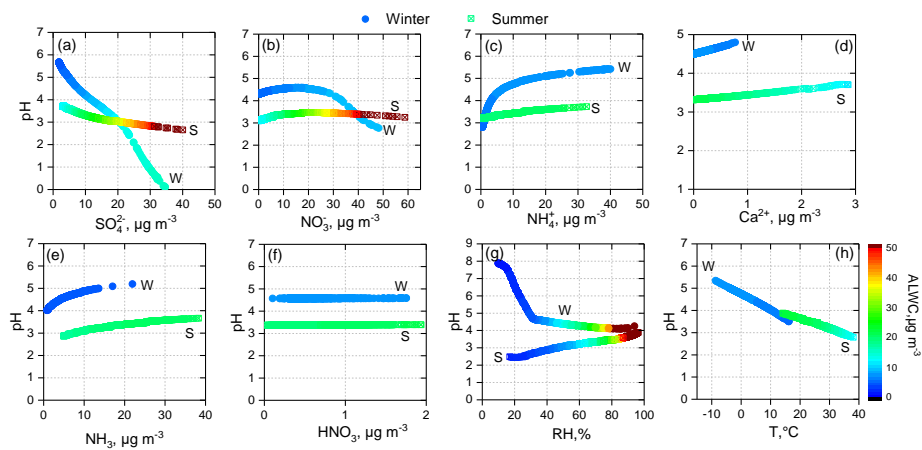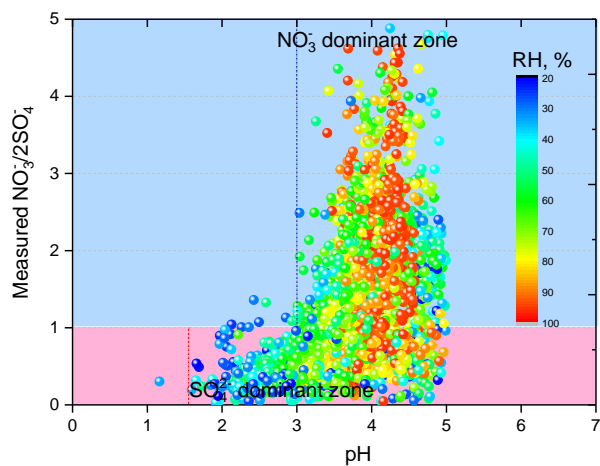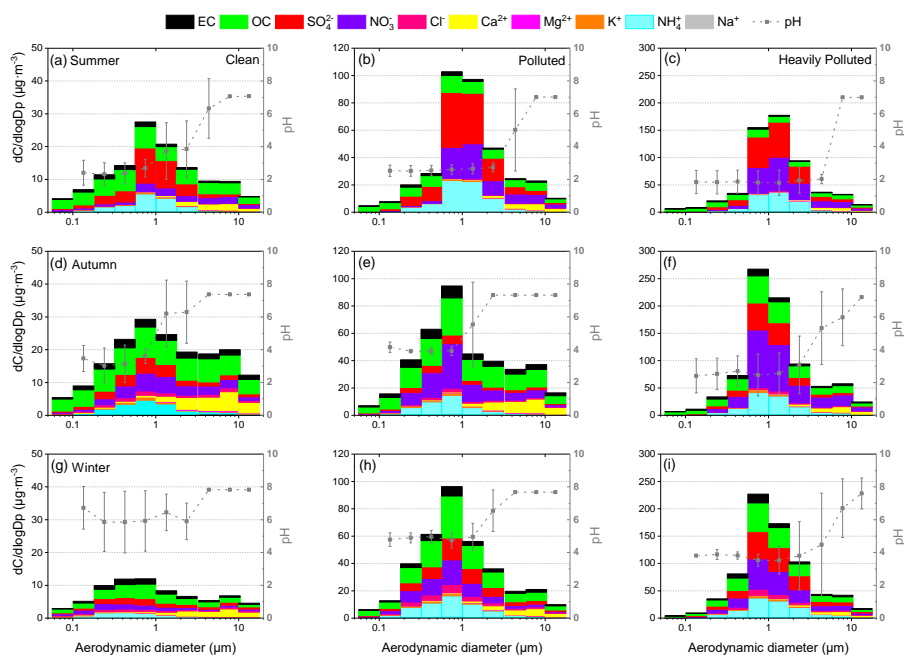
724

725   **Figure 9.**

726

727

Figure 10.